



Published in final edited form as:

*J Atmos Sol Terr Phys.* 2016 June ; 143-144: 8–13. doi:10.1016/j.jastp.2016.03.002.

## Comparison of DMSP and SECS region-1 and region-2 ionospheric current boundary☆

J.M. Weygand<sup>a,b,\*</sup> and S. Wing<sup>c</sup>

<sup>a</sup>Institute of Geophysics and Planetary Physics, University of California Los Angeles, Los Angeles, CA, USA

<sup>b</sup>Department of Earth, Planetary, and Space Sciences, University of California Los Angeles, Los Angeles, CA, USA

<sup>c</sup>Johns Hopkins University Applied Physics Laboratory, Laurel, MD, USA

### Abstract

The region-1 and region-2 boundary has traditionally been identified using data from a single spacecraft crossing the auroral region and measuring the large scale changes in the cross track magnetic field. With data from the AUTUMN, CANMOS, CARISMA, GIMA, DTU MGS, MACCS, McMAC, STEP, THEMIS, and USGS ground magnetometer arrays we applied a state-of-art technique based on spherical elementary current system (SECS) method developed by Amm and Viljanen (1999) in order to calculate maps of region-1 and region-2 current system over the North American and Greenland auroral region. Spherical elementary current (SEC) amplitude (proxy for vertical currents) maps can be inferred at 10 s temporal resolution,  $\sim 1.5^\circ$  geographic latitude (Glat), and  $3.5^\circ$  geographic longitude (Glon) spatial resolution. We compare the location of the region-1 and region-2 boundary obtained by the DMSP spacecraft with the region-1 and region-2 boundary observed in the SEC current amplitudes. We find that the boundaries typically agree within  $0.2^\circ \pm 1.3^\circ$ . These results indicate that the location of the region-1 and region-2 boundary can reasonably be determined from ground magnetometer data. The SECS maps represent a value-added product from the magnetometer database and can be used for contextual interpretation in conjunction with other missions as well as help with our understanding of magnetosphere-ionosphere coupling mechanisms using the ground arrays and the magnetospheric spacecraft data.

### 1. Introduction

The ionospheric region-1 and region-2 currents (i.e., Birkeland currents) run parallel to the Earth's magnetic field connecting the Earth's ionosphere with the magnetosphere and they are the ionospheric projection of different magnetospheric regions. The nightside region-1 currents located in the high latitudes in the auroral oval are believed to be driven by magnetospheric convection in the plasma sheet (Sonnerup, 1980; Bythrow et al., 1981).

\*Corresponding author at: Institute of Geophysics and Planetary Physics, University of California Los Angeles, Los Angeles, CA, USA. jweygand@igpp.ucla.edu (J.M. Weygand).

☆UCLA Institute of Geophysics and Planetary Physics Department of Earth, Planetary, and Space Science.

Moreover, Wing et al. (2010) shows that while region-1 currents near noon are frequently located at the boundary layer and on open-field lines and region-1 currents near dawn and dusk are frequently located in the closed field lines that map to the plasma sheet. The magnetic field lines intersecting the region-1 current system can be associated with the plasma sheet, plasma sheet boundary layer, and low latitude boundary layer. These magnetic field lines are more stretched in the magnetotail region. The region-2 currents located at the low latitudes of the auroral oval are believed to be generated by pressure gradients in the inner magnetosphere (Vasiliunas, 1970; Southwood, 1977; Harel et al., 1981). The magnetic field lines intersecting the region-2 current system can be magnetically field line mapped to the plasmasphere and to the region between the plasmasphere and the plasma sheet. These region-2 magnetic field lines are more dipole like in nature. Knowing the location of the boundary between the region-1 and region-2 current system helps us identify the boundary between the plasma sheet and the inner magnetosphere. Furthermore, Jiang (2013) and Jiang et al. (2015) has shown the pre-substorm onset auroral arc is within  $\sim 1^\circ$  of the boundary between the region-1 and region-2 field aligned currents, but the auroral arc typically sits within upward field aligned currents and that the magnetospheric counter part of the pre-onset auroral arc is a flow shear within the plasma sheet.

Knowing the location of the boundary between the region-1 and region-2 current system also helps roughly identify the particle precipitation regions. The studies of Ohtani et al. (2010) and Contents lists available at ScienceDirect Wing et al. (2010) demonstrated with the Defense Meteorological Satellite Program (DMSP) spacecraft distinct differences in the particle precipitation associated with the region-1 and region 2 currents. Specifically, some of the features Ohtani et al. (2010) and Wing et al. (2010) showed are: (1) the maximum energy flux of ion precipitation occurs inside the region-2 currents irrespective of magnetic local time. (2) The region-2 currents consist of precipitation from the central plasma sheet (CPS) and boundary plasma sheet (BPS) in the morning and from the CPS, BPS, and inner magnetosphere in the afternoon. (3) The occurrence distributions of the most equatorward and poleward electron acceleration events indicate that monoenergetic electron precipitation is mostly confined in the upward region-1 current in dusk to midnight sector. (4) Region-1 currents mostly map to the BPS on closed magnetic field lines in morning and afternoon. (5) Finally, the transition between structured and unstructured electron precipitation typically occurs around the region-1 and region-2 boundary.

Low earth orbiting spacecraft in polar orbits, such as the DMSP spacecraft, observe the boundary between the region-1 and region-2 current systems as a sharp change in the cross track component of the magnetic field (Wing et al., 2010). However, the DMSP spacecraft and any other spacecraft in a similar orbit with a magnetometer only obtain a one dimension cut of the auroral oval and a single location of the region-1 and region-2 boundary. Furthermore, it is assumed that the region-1 and region-2 currents system is static or slowly varying to obtain the location of the region-1 and region-2 boundary within the timescale of several minutes that it takes DMSP to cross the two regions. On the other hand, a two dimensional picture of the region-1 and region-2 currents system and its boundary can provide context for both magnetospheric spacecraft and ionospheric observations such as auroral images, particle precipitation, and ionospheric radar measurements. Furthermore, a two dimensional picture of the region-1 and region-2 currents system can help with our

understanding of magnetosphere–ionosphere coupling mechanisms using the ground arrays and magnetospheric spacecraft data.

A two dimensional picture of the ionospheric currents can be derived with an array of well spaced ground magnetometers. The spherical elementary current systems (SECS) method (Amm and Viljanen, 1999), which has been regularly applied to the International Monitor for Auroral Geomagnetic Effects (IMAGE) ground magnetometer array, can calculate the equivalent ionospheric currents, the approximate region-1 and region-2 currents, and the boundary between the region-1 and region-2 currents. The SECS technique defines two elementary current systems: a divergence-free elementary system with currents that flow entirely within the ionosphere and a curl-free system whose divergences represent the currents normal to the ionosphere. For uniform ionospheric conductances, the divergence-free and curl-free current density components equal the Hall and Pedersen current density components, respectively. The superposition of these two elementary current systems with different weights (scaling factors) can reproduce any vector field on a sphere. If it is known a priori that the vector field is curl-free or divergence-free, then only one set of basis functions is needed, and thus 50% of the free coefficients (those associated with the other current system) can be eliminated. One of the important features of this technique is it requires no integration time of the magnetometer data. Recently, the technique has been applied to the magnetometers located in North America and Greenland (Weygand et al., 2011, 2012, 2015).

In this study we mainly focus on the SEC current amplitudes, which are a proxy for the vertical currents. The current amplitudes are calculated from the curl of the equivalent ionospheric currents. To obtain these results we make two assumptions. The first assumption is that the Hall to Pedersen conductance ratio is constant:  $\alpha = \Sigma_H / \Sigma_P = \text{constant}$  where  $\Sigma_H$  and  $\Sigma_P$  are the height integrated Hall and Pedersen conductivities. The second assumption is that  $(\nabla \Sigma_H \times \vec{E})_r = 0$ , where  $\vec{E}$  is the convection electric field. From these two assumptions the current amplitudes can be written as:

$$j_{df,r} = \nabla \cdot \vec{J} = -\frac{1}{\alpha} (\nabla \times \vec{J}_{df})$$

where  $\vec{J}_{df}$  is the divergence free currents (equivalent currents) and  $j_{df,r}$  is the current amplitude. For more details see Amm et al. (2002), Juusola et al. (2009) and Vanhamäki and Amm (2011).

The objective of this study is to compare the location of the boundary between the region-1 and region-2 current system identified in the DMSP auroral passes with the DMSP fluxgate magnetometer (Rich et al., 1985) with the boundary between the region-1 and region-2 current system observed with the SECS current amplitudes. In the next section we will review the data and methodology. In the third section we will present our results using over 100 region-1 and region-2 boundaries and in the last two sections we will discuss the importance of our results and summarize.

## 2. Data

The data for this study come from two distinct sources: the DMSP magnetometer from multiple DMSP spacecraft and the SECS current amplitudes, which are derived from ten ground magnetometer arrays in North America and Greenland. The DMSP satellites are Sun synchronous satellites in nearly circular polar orbit at an altitude of about 830 km and with an orbital period of approximately 101 min. The spacecraft are typically in one of two orbital planes: approximately dawn-dusk and pre-noon-pre-midnight. In this study we will use data from the dawn to dusk passes in the northern hemisphere. We use the dawn to dusk passes because this field aligned current system is simple and typically consists of an interval of an upward current region and a downward current region. The DMSP magnetic field experiment, the Special Sensor Magnetometer (*SSM*), consist of triaxial fluxgate magnetometer with a range of  $\pm 65,535$  nT, a resolution of 2 nT, and a temporal resolution of 1 s (Rich et al., 1985).

For this study we have obtained data from 10 different ground magnetometer arrays: AUTUMN (Athabasca University THEMIS UCLA Magnetometer Network (<http://autumn.athabascau.ca/>), CANMOS (CANadian Magnetic Observatory System) (<http://geomag.nrcan.gc.ca/obs/canmos-eng.php>), CARISMA (Canadian Array for Real time Investigations of Magnetic Activity) (Mann et al., 2008), GIMA (Geophysical Institute Magnetometer Array) (<http://www.asf.alaska.edu/program/gdc/project/magnetometer>), Technical University of Denmark (DTU) Magnetometer Ground Stations in Greenland (<http://www.space.dtu.dk/MagneticGroundStations.aspx>), MACCS (Magnetometer Array for Cusp and Cleft Studies) (Engebretson et al., 1995), McMAC (Mid-continent magnetoseismic chain) (Chi et al., 2013), the STEP (Solar-Terrestrial Energy Program) magnetometer array (<http://step-p.dyndns.org/~khay/>), and THEMIS GMAG (Time History of Events and Macroscale Interactions During Substorms Ground MAGnetometers) (Russell et al., 2008), and USGS (United States Geophysical Survey) (<http://www.usgs.gov/>). Many of the ground magnetometer arrays share some stations. All of the data from GIMA, MACCS, and Greenland stations used in this study can be obtained from the THEMIS GMAG online data archive, while the rest were obtained from the original provider. In total we have the potential of obtaining data from nearly 100 different stations at this time. We have not included the Greenland stations on the East coast because these stations are located far from the rest of the ground magnetometers. Fig. 1 of Weygand et al. (2015) displays the distribution of the stations used in this study.

The SECS are calculated with the available ground magnetometer data. The number of available stations may change from day to day due to data gaps, changes in baseline, and measurement errors. The spatial resolution of the SECS current amplitudes is about  $1.5^\circ$  in geographic latitude ( $\sim 161$  km) and about  $3.5^\circ$  degrees geographic longitude (roughly 173 km). The temporal resolution for this data set is 10 s. More details on the calculation of the SECS and the description of the SECS over North America and Greenland can be found in Amm and Viljanen (1999) and Weygand et al. (2011).

### 3. Procedure and Observations

The first step is to select intervals with DMSP magnetometer data that can be confidently identified with region-1 and region-2 boundaries. The DMSP magnetometer data intervals are selected visually and we have specifically selected events from dawn and dusk side crossing. All the events in this study occurred between December 2007 and April 2008 when *ground magnetometer data are available from which the SECS are derived*. Dawn and dusk side crossings are selected because the region-1 and region-2 currents system is relatively simple. These regions typically consist of a single downward and upward current system and they are less complicated. For example, Wing et al. (2010) shows that large scale two current sheet pattern, i.e., region-1 and region-2 currents, occurs 80% of the time near dawn and dusk. On the other hand, the Harang region in the night side sector and the dayside cusp region near noon can exhibit more complicated current patterns having more than two current sheets (Iijima and Potemra, 1976). Approximately 75% of the dawn and dusk side DMSP crossings were rejected due to poor clarity of the region-1 and region-2 boundary in the DMSP magnetometer data and/or the SECS data. By poor clarity of the region-1 and region-2 boundary we mean that multiple regions of upward and downward current sheets were present in the DMSP magnetometer data and/or SECS data making a clear identification of the region-1 and region-2 difficult. Also, a number of events were rejected when the SECS appeared to be patches of upward and downward current amplitudes and not two simple clear bands of region-1 and region-1 current.

Fig. 1 shows an example of a duskside crossing of the auroral oval. The top panel displays the DMSP  $B_y$  component of the magnetic field, which points radial inward for the DMSP magnetometer. The middle panel shows the DMSP  $B_z$  component, which is the cross track component of the magnetic field and basically points westward. The middle panel shows the downward region-2 current and the upward region-1 current that have been labeled between the gray vertical lines. The middle vertical gray line at  $64^\circ$  geographic latitude (GLat) marks the DMSP region-1 and region-2 boundary. The region-1 and region-2 boundary is defined at the peak in the  $B_z$  component of the magnetic field. For each boundary we can obtain a location and the time at which DMSP crosses the boundary. The bottom panel of Fig. 1 shows the SECS current amplitudes given as black '+' symbols. The plotted values are the closest SECS currents in time and space at the foot point of the DMP spacecraft. Positive currents are upward and negative currents are downward. The direction of the region-1 (upward) and region-2 (downward) currents are as expected in the duskside auroral oval (Iijima and Potemra, 1976). The black diamond at about  $64^\circ$  GLat marks the SECS region-1 and region-2 boundary. This boundary was determined by linearly interpolating the SECS data between values at '+' symbols to find the location of 0 Amp crossing between the positive and negative current values. The time at which the SECS boundary is defined as the time of the SEC map closest to the time when the foot point of the DMP spacecraft crosses the region-1 and region-2 boundary. Since the resolution of the SECS is 10 s, the difference between the time when DMSP crosses the region-1 and region-2 boundary and the time when we define the location of the SECS region-1 and region-2 boundary can be up to 5 s. This example in Fig. 1 shows there is little or no difference between the DMSP region-1 and region-2 boundary and the SECS boundary.

Fig. 2 display the two dimension SECs over North America and Greenland. The red “+s” and blue squares indicate upward and downward currents, respectively. The key is given in the lower right corner. The black north–south line on the right side of the image indicates local midnight. The blue squares extending from Alaska across Canada to the southern end of Hudson Bay ( $\sim 55^\circ$  GLat,  $\sim 270^\circ$  GLon) display where the region-2 current flows into the ionosphere and the red crosses poleward of the blue indicate where the region-1 current flows out of the ionosphere. The Harang region is located on the eastern side of the Hudson bay. The lime green line on the west coast indicates the path of the DMSP spacecraft from low latitude to high latitude and the mauve dot indicates the region-1 and region-2 boundary identified with the DMSP magnetometer data, which sits at the region-1 and region-2 SECs boundary between the red and blue symbols.

In the last example we showed a boundary crossing on the duskside auroral oval. In Fig. 3 we show a dawnside auroral oval crossing. The format of this figure is the same as Fig. 1 and in this event DMSP F17 traverses from high latitudes to low latitudes. In the bottom panel the SECs values are the opposite orientation of those SECs values in Fig. 1 and as expected for the dawnside region-1 and region-2 currents. The region-1 and region-2 boundary in the DMSP data (middle panel) occurs at  $58.7^\circ$  GLat and at about  $58^\circ$  GLat in the SECS currents. Fig. 4 shows the corresponding two dimensional spherical elementary current system. This figure has the same format as Fig. 2 and DMSP F17 traverses from high latitudes to low latitudes. The mauve dot again lies between the blue downward region-1 current system and the red upward region-2 current system at about  $58^\circ$  GLat and  $105^\circ$  GLon.

#### 4. Discussion and Conclusions

In total we identified 110 events with near simultaneous region-1 and region-2 boundary observations (to within 5 s) in both the DMSP/SSM data and SECS data. Sixty-three of these events occurred in the duskside auroral oval sector and the remaining 47 occur in the dawnside auroral oval sector. In Fig. 5 we show a histogram of the difference between the SECS region-1 and region-2 boundary and the DSMP/SSM region-1 and region-2 boundary for all 110 events. Along the  $x$ -axis is the difference in geographic latitude and the bin size is  $0.5^\circ$ . Located in the upper right corner are the mean, median, and standard deviation of the differences in latitude. For all the events in this study the mean (and median) difference is  $-0.2^\circ \pm 1.3^\circ$ . Recall that the spatial resolution of the SECS current amplitudes is  $1.5^\circ$  in latitude, which means using the SECS method we are able to locate on average the region-1 and region-2 boundary within the spatial resolution of the currents. We also examined the skewness and kurtosis of the distribution and find that the skewness is  $-0.2$  and kurtosis is  $3.6$ . These two values indicate that the distribution is approximately symmetric (skewness of 0) and nearly Gaussian (kurtosis of 3).

Fig. 5 and the standard deviation of the histogram indicate that large differences between the SECS region-1 and region-2 boundary and the DSMP/SSM region-1 and region-2 boundary do occur. In Figs. 6 and 7 we investigate whether there is a dawn or dusk side preference for the large differences between the SECS region-1 and region-2 boundary and the DSMP/SSM region-1 and region-2 boundary. The format and scales of these figures is the same as Fig. 5

and in both figures it is clear that the mean, median, and standard deviation are nearly the same. Furthermore, the skewness and kurtosis of these distributions are also similar to the skewness and kurtosis in Fig. 5, which indicates that the difference in latitude is not related to the dawn or dusk sector.

Figs. 5–7 demonstrate that the mean difference between the SECS region-1 and region-2 boundary and the DSMP/SSM region-1 and region-2 boundary is small, but larger differences up to  $3^\circ$  occur. We have determined that these differences are not correlated with the level of geomagnetic activity (results not shown). We can also state that the larger differences in latitude are not related to auroral dynamics. Hargreaves et al. (1975) has shown that the ionospheric currents in the auroral oval during active periods drift equatorward with speeds on the order of 200–500 m/s. The largest time difference between the identification of the DSMP/SSM region-1 and region-2 boundary and the SECS region-1 and region-2 boundary is 5 s, which translates to at most a shift in the region-1 and region-2 boundary location of about 2.5 km and much smaller than the spatial resolution of both the SECS and DMSP data.

We have demonstrated that the mean difference between the SECS region-1 and region-2 boundary and the DSMP/SSM region-1 and region-2 boundary is  $-0.2^\circ \pm 1.3^\circ$  for dawn and dusk side crossing of the DMSP spacecraft when the region-1 and region-2 currents system is relatively simple. In this study we define simple as a single pronounced *band* of upward and downward current and not multiple crossings of strong upward and downward currents or patches of upward and downward currents. Prior particle precipitation studies, such as Ohtani et al., (2010) and Wing et al. (2010), have shown differences in the particle precipitation can vary relative the region-1 and region-2 boundary. Specifically, the transition from structured to unstructured particle precipitation tends to occur at the region-1 and region-2 boundary and the maximum energy flux of ion precipitation occurs within the region-2 current irrespective of the magnetic local time. The SECS method applied to the magnetometer arrays over North American can show the region-1 and region-2 boundary over approximately 8 h of local time. The SECS method can provide contextual interpretation for particle precipitation measurements and the magnetosphere-ionosphere current system in conjunction with other missions such as the SuperDARN radar measurements, all sky images, and AMPERE current densities.

## Acknowledgments

We thank the many different groups operating magnetometer arrays for providing data for this study including: the THEMIS UCLA magnetometer network (Ground-based Imager and Magnetometer Network for Auroral Studies) is funded through NSF grant AGS-1004736. AUTUMNX magnetometer network is funded through the Canadian Space Agency/Geospace Observatory (GO) Canada program Athabasca University, Centre for Science/Faculty of Science and Technology. The Canadian Space Science Data Portal is funded in part by the Canadian Space Agency contract numbers 9F007-071429 and 9F007-070993. The Canadian Magnetic Observatory Network (CANMON) is maintained and operated by the Geological Survey of Canada – <http://gsc.nrcan.gc.ca/geomag>. The Magnetometer Array for Cusp and Cleft Studies (MACCS) array is supported by US National Science Foundation grant ATM-0827903 to Augsburg College. The McMAC Project is sponsored by the Magnetospheric Physics Program of National Science Foundation through grant AGS-0245139 and maintained by Dr. Peter Chi. We would like to would like to thank the following: Jürgen Matzka for calibrating the DTU magnetometers; M. J. Engebretson, D. Murr, and E.S. Steinmetz at Augsburg College; and the MACCS team. The Solar and Terrestrial Physics (STEP) magnetometer file storage is at Department of Earth and Planetary Physics, University of Tokyo and maintained by Dr. Kanji Hayashi (hayashi@grl.s.u-tokyo.ac.jp). This study was made possible by NASA THEMIS grant NAS5-02099 at UCLA. We also acknowledge NASA HiDEE award number NNX14AJ77G. Simon Wing

acknowledges supports from NSF Grant AGS-1058456 and NASA Grants (NNX13AE12G and NNX15AJ01G). We thank the CSA for logistical support in fielding and data retrieval from the GBO stations. The Alaska and Greenland portions of the GBO network are supported by NSF through grant 1004736. We would also like to thank Dr. M. G. Kivelson, Dr. K.K. Khurana, Dr. R.L. McPherron, Dr. R.J. Strangeway, Dr. V. Angelopoulos, and Dr. R.J. Walker for their invaluable input.

## References

- Amm O, Engebretson MJ, Hughes T, Newitt L, Viljanen A, Watermann J. A traveling convection vortex event study: Instantaneous ionospheric equivalent currents, estimation of field-aligned currents, and the role of induced currents. *J. Geophys. Res.* 2002; 107:1334. <http://dx.doi.org/10.1029/2002JA009472>.
- Amm O, Viljanen A. Ionospheric disturbance magnetic field continuation from the ground to the ionosphere using spherical elementary current systems. *Earth Planets Space.* 1999; 51:431.
- Bythrow P, Heelis RA, Hanson WB, Power RA, Hoffman RA. Observational evidence for a boundary layer source of dayside region 1 field—aligned currents. *J. Geophys. Res.* 1981; 86:5577.
- Chi PJ, Engebretson MJ, Moldwin MB, Russell CT, Mann IR, Hairston MR, Reno M, Goldstein J, Winkler LI, Cruz-Abeyro JL, Lee D-H, Yumoto K, Dalrymple R, Chen B, Gibson JP. Sounding of the plasmasphere by Mid-continent MAGnetoseismic Chain (McMAC) magnetometers. *J. Geophys. Res. Space Phys.* 2013; 118:3077–3086. <http://dx.doi.org/10.1002/jgra.50274>.
- Engebretson MJ, Hughes WJ, Alford JL, Zesta E, Cahill LJ Jr, Arnoldy RL, Reeves GD. MACCS observations of the spatial extent of broadband ULF magnetic pulsations at Cusp/Cleft latitudes. *J. Geophys. Res.* 1995; 100:19371.
- Harel M, Wolf RA, Spiro RW, Reiff PH, Chen CK, Burke WJ, Rich FJ, Smiddy M. Quantitative simulation of a magnetospheric substorm 2. Comparison with observations. *J. Geophys. Res.* 1981; 86:2242.
- Hargreaves JK, Chivers HJA, Axford WJ. Development of substorm in auroral radio absorption. *Planet Space Sci.* 1975; 23:905–911.
- Iijima T, Potemra T. Field-aligned currents in the dayside cusp observed by Triad. *J. Geophys. Res.* 1976; 81:5971–5979.
- Jiang F, Kivelson MG, Strangeway RJ, Khurana KK, Walker RJ. Ionospheric flow shear associated with the preexisting auroral arc: a statistical study from FAST spacecraft data. *J. Geophys. Res.* 2015; 120:5194–5213. <http://dx.doi.org/10.1002/2013JA019255>.
- Jiang, F. Ph.D. dissertation. University of California; Los Angeles: 2013. The Magnetospheric Source of the Pre-existing Auroral Arc.
- Juusola L, Nakamura R, Amm O, Kauristie K. Conjugate ionospheric equivalent currents during bursty bulk flows. *J. Geophys. Res.* 2009; 114:A04313. <http://dx.doi.org/10.1029/2008JA013908>.
- Mann IR, Milling DK, Rae IJ, Ozeke LG, Kale A, Kale ZC, Murphy KR, Parent A, Usanova M, Pahud DM, Lee E-A, Amalraj V, Wallis DD, Angelopoulos V, Glassmeier K-H, Russell CT, Auster H-U, Singer HJ. The upgrade CARISMA magnetometer array in the THEMIS era. *Space Sci. Rev.* 2008; 141:413–451. <http://dx.doi.org/10.1007/s11214-008-9457-6>.
- Ohtani S, Wing S, Newell PT, Higuchi T. Locations of night-side precipitation boundaries relative to R2 and R1 currents. *J. Geophys. Res.* 2010; 115:A10233. <http://dx.doi.org/10.1029/2010JA015444>.
- Rich, FJ., Hardy, DA., Gussenhoven, MS. *Eos Trans. Vol. 66. AGU; 1985. Enhanced ionosphere-magnetosphere data from the DMSP satellites; p. 513*
- Russell CT, Chi PJ, Dearborn DJ, Ge YS, Kuo-Tiong B, Means JD, Pierce DR, Rowe KM, Snare RC. THEMIS ground-based magnetometers. *Space Sci. Rev.* 2008; 141:389–412. <http://dx.doi.org/10.1007/s11214-008-9337-0>.
- Sonnerup BUÖ. Theory of the low-latitude boundary layer. *J. geophys. Res.* 1980; 85:2017.
- Southwood DJ. The role of hot plasma in magnetospheric convection. *J. Geophys. Res.* 1977; 82(35): 5512–5520. <http://dx.doi.org/10.1029/JA082i035p05512>.
- Vanhamäki H, Amm O. Analysis of ionospheric electrodynamic parameters on mesoscales – a review of selected techniques using data from ground-based observation networks and satellites. *Ann. Geophys.* 2011; 29:467–491. <http://dx.doi.org/10.5194/angeo-29-467-2011>.

- Vasiliunas, VM. Mathematical models of magnetospheric convection and its coupling to the ionosphere. In: McCormac, BM., editor. *Particles and Fields in the Magnetosphere*. Holland, Higham, Mass: 1970. p. 60-71.
- Weygand JM, Amm O, Viljanen A, Angelopoulos V, Murr D, Engebretson MJ, Gleisner H, Mann I. Application and validation of the spherical elementary currents systems technique for deriving ionospheric equivalent currents with the North American and Greenland ground magnetometer arrays. *J. Geophys. Res.* 2011; 116 <http://dx.doi.org/10.1029/2010JA016177>.
- Weygand JM, Amm O, Angelopoulos V, Milan SE, Grocott A, Gleisner H, Stolle C. Comparison between SuperDARN flow vectors and equivalent ionospheric currents from ground magnetometer arrays. *J. Geophys. Res.* 2012; 117:A05325. <http://dx.doi.org/10.1029/2011JA017407>.
- Weygand, JM., Kivelson, MG., Angelopoulos, V., Frey, HU., Rodriguez, JV., Redmon, R., Barker-Tvedtnes, J., Grocott, A., Amm, O., Xing, X. An interpretation of spacecraft and ground based observations of multiple omega bands events. *J. Atmos. Sol-Terr. Phys.* 2015. <http://dx.doi.org/10.1016/j.jastp.2015.08.014>
- Wing S, Ohtani S, Newell PT, Higuchi T, Ueno G, Weygand JM. Dayside field-aligned current source regions. *J. Geophys. Res.* 2010; 115:A12215. <http://dx.doi.org/10.1029/2010JA015837>.

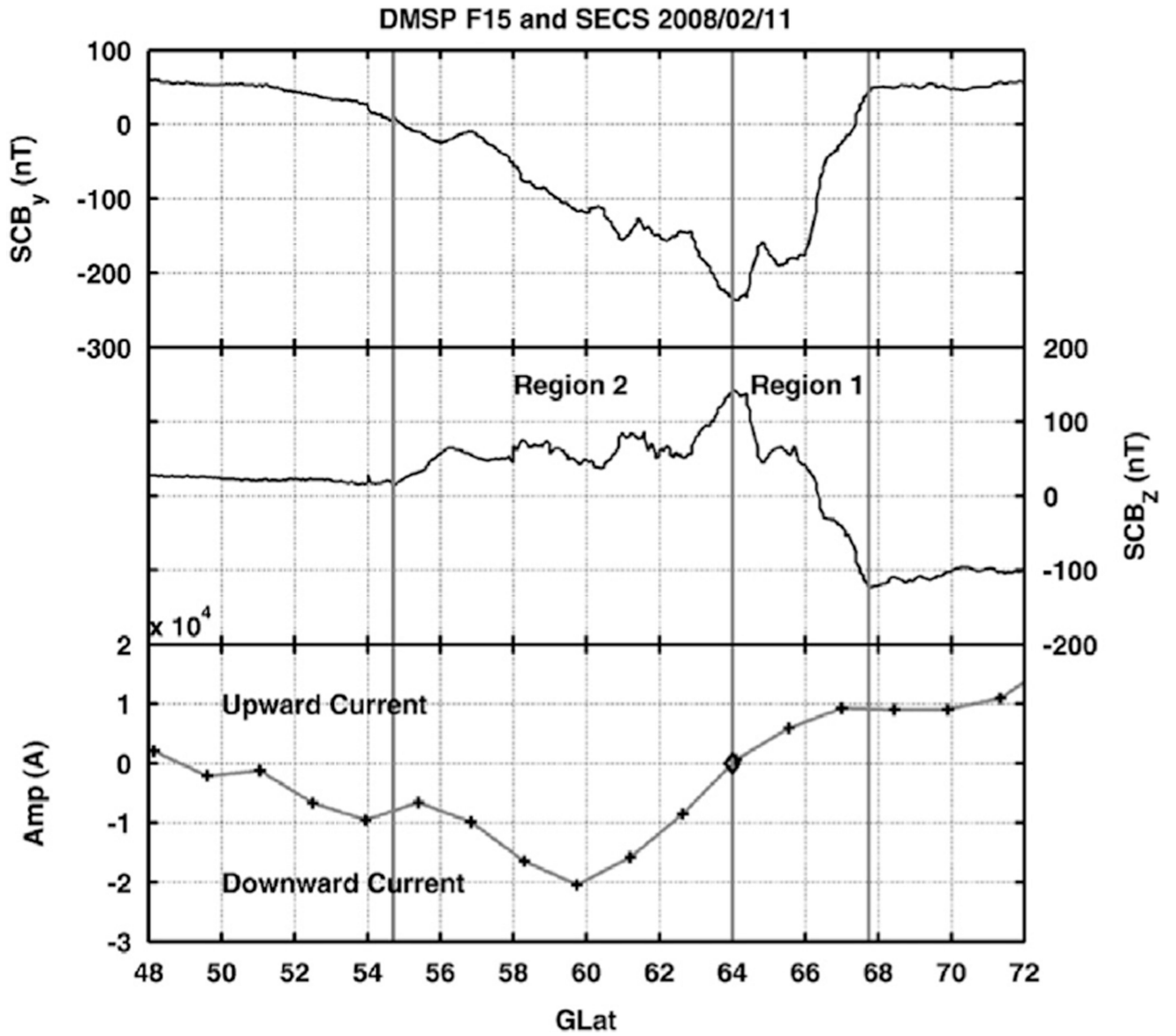


**Fig. 1.** Region-1 and region-2 duskside boundary crossing. The top panel shows the DMSF F15  $B_y$  radial inward component and the second panels displays the DMSF cross track  $B_z$  component. The bottom panel displays the SECS current amplitudes, where the '+' gives the SECS value closest to the foot point of the DMSF spacecraft. The gray vertical lines delineate the region-1 and region-2 borders and the middle vertical lines marks the region-1 and region-2 boundary. The diamond in the bottom panel at 64° GLat marks the SECS region-1 and region-2 boundary.

## THEMIS SECs Scaling Factors: 11-Feb-2008 02:34:00

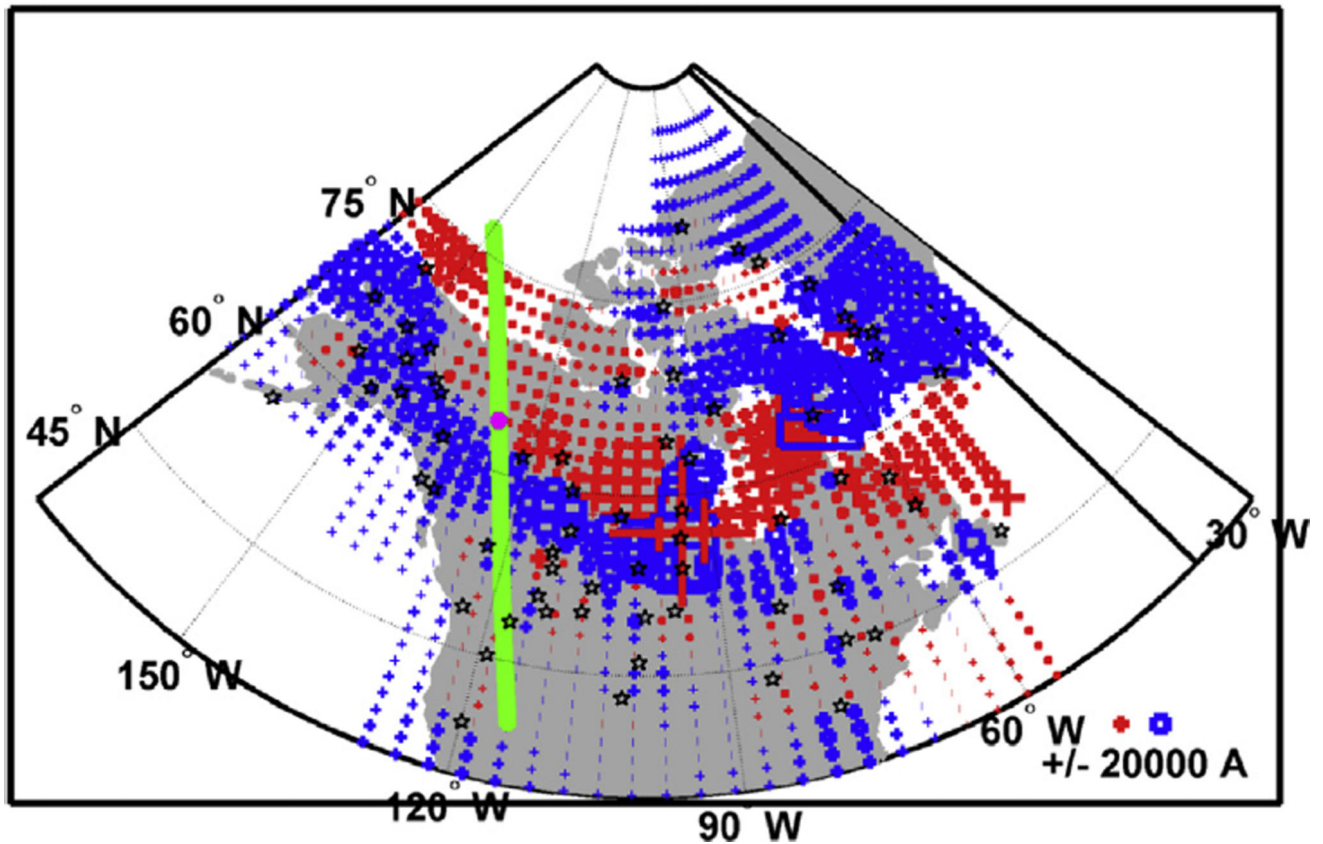


**Fig. 2.**

SECs two dimension current system over North America and Greenland. The red '+' symbols indicates upward current amplitudes and the blue squares indicate the downward current amplitudes. The black line over Greenland marks local midnight. The green light shows the path of the DMSP spacecraft from low latitude to high latitude and the mauve dot marks the DMSP region-1 and region-2 boundary, which is co-located with the SECS boundary. The black stars mark the ground magnetometers used to calculate the current system. (For interpretation of the references to color in this figure, the reader is referred to the web version of this article.)

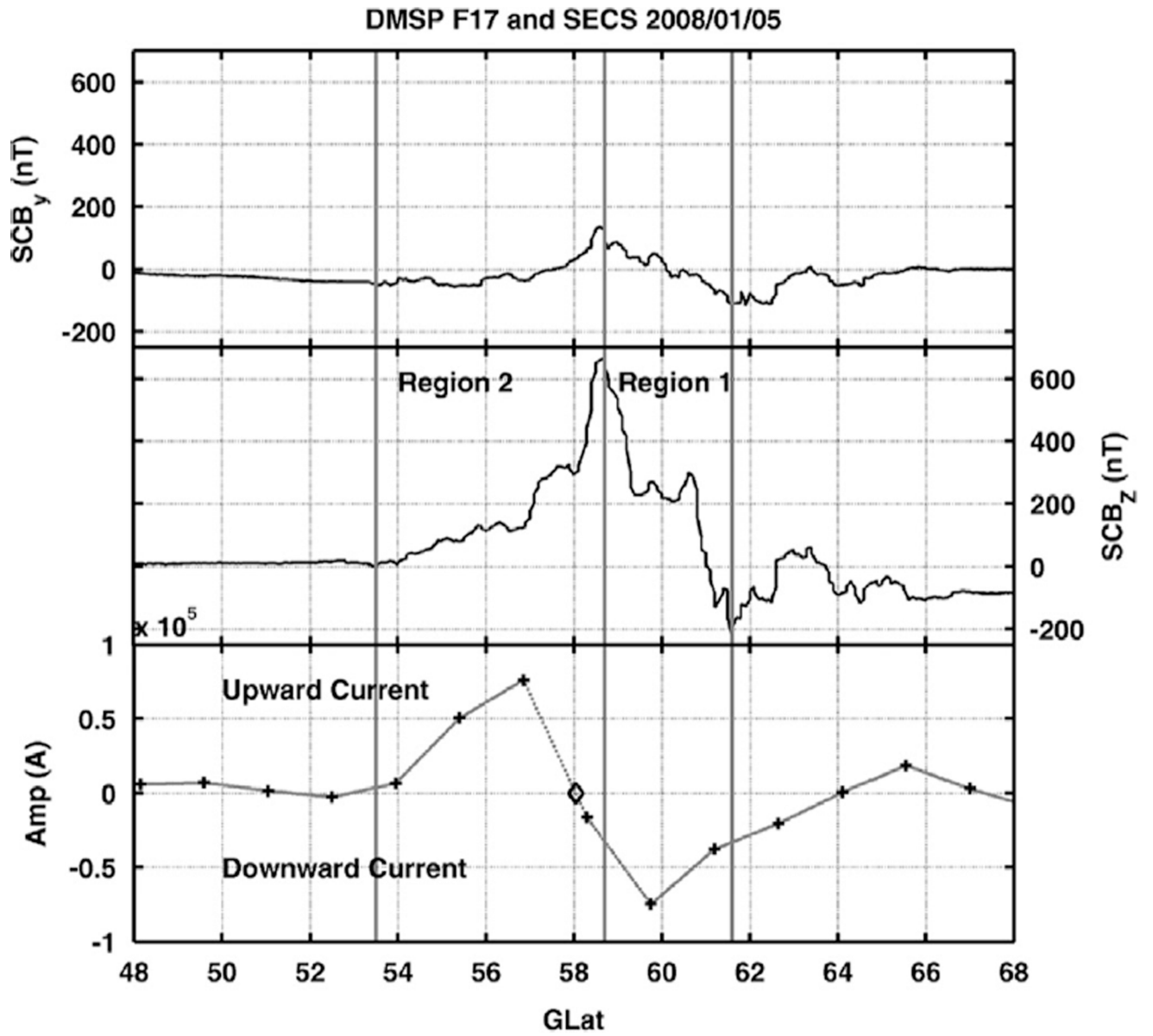
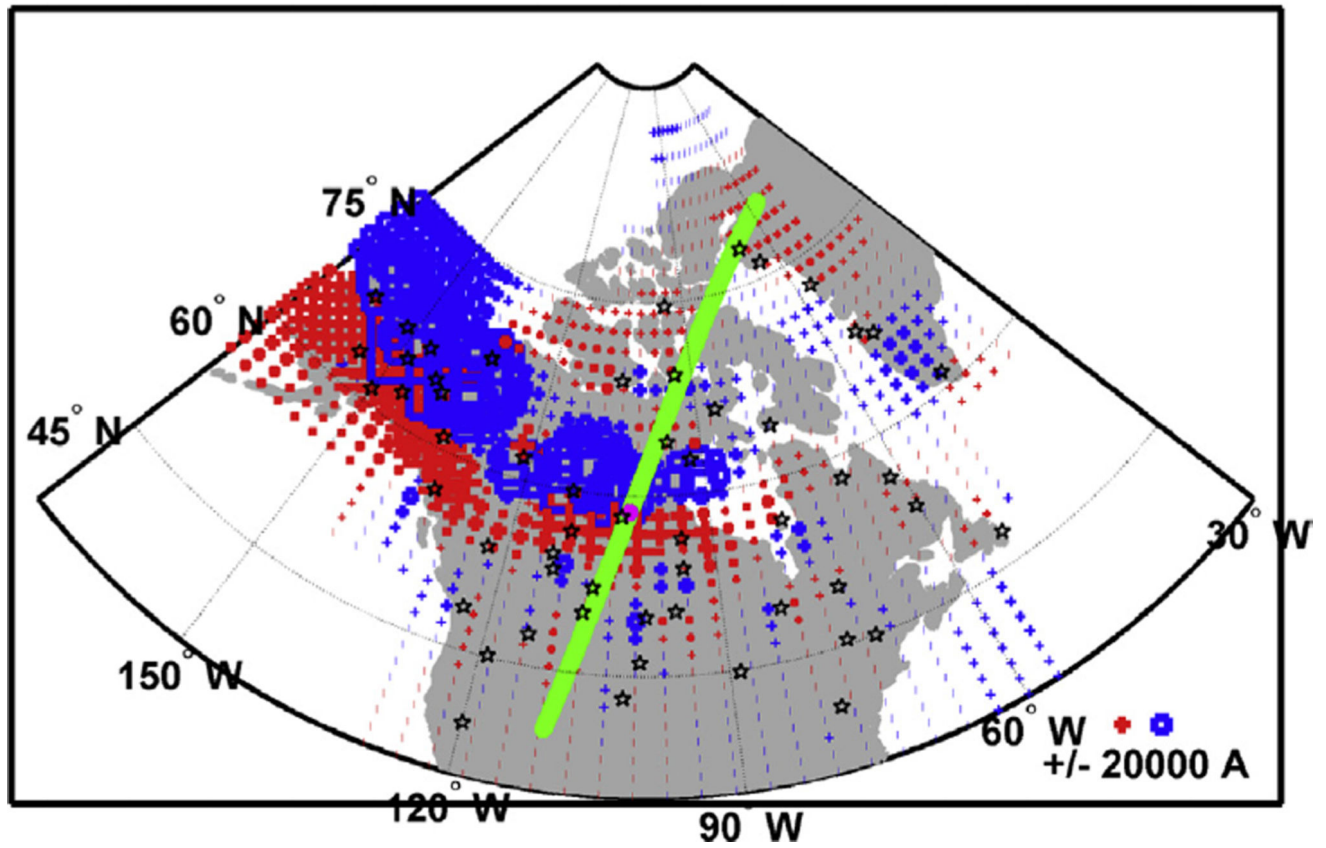
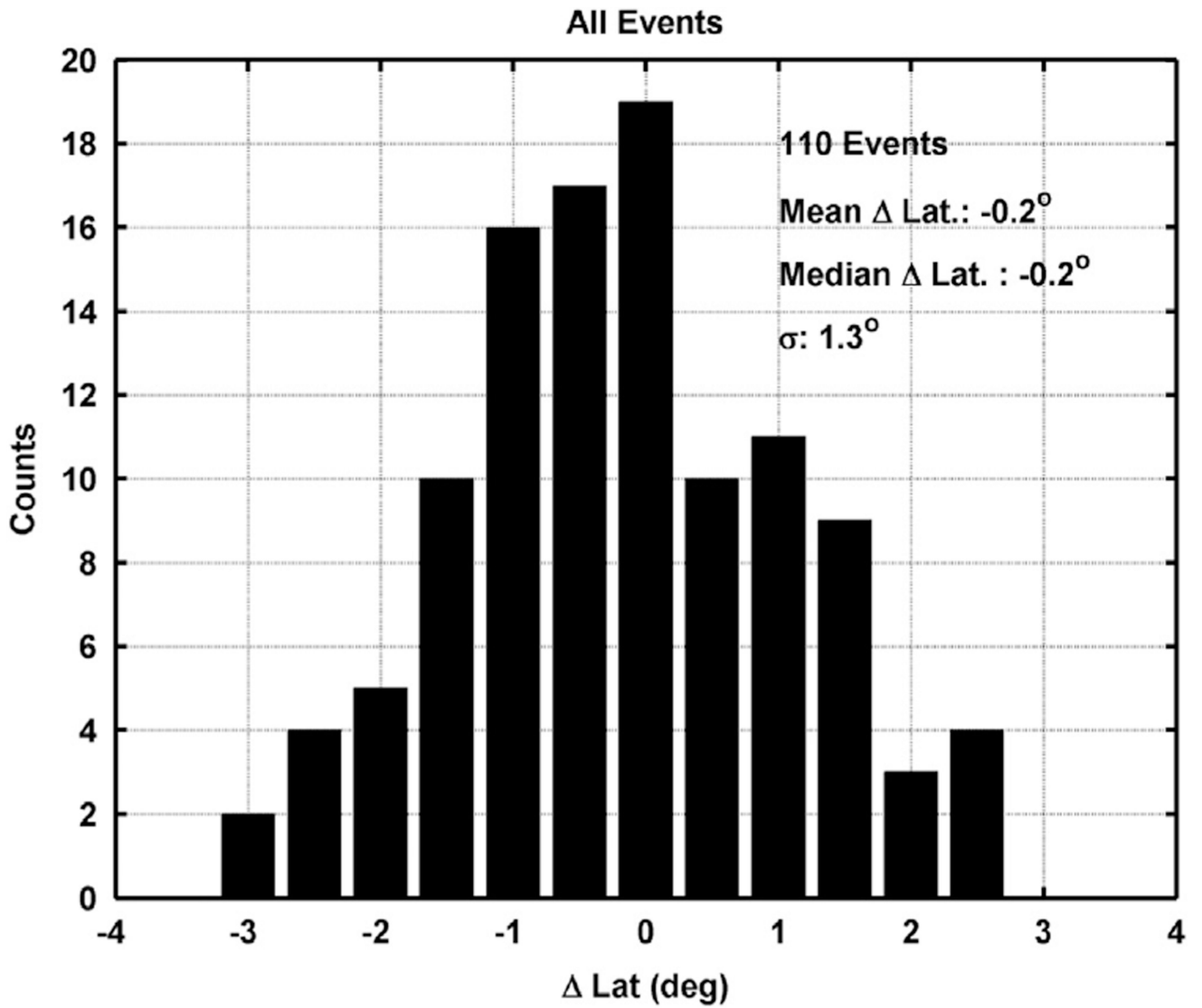


Fig. 3. Region-1 and region-2 dawnside boundary crossing of DMSP F17. This figure has the same format as Fig. 1.

## THEMIS SECs Scaling Factors: 05-Jan-2008 13:22:00



**Fig. 4.**  
This figure has the same format as Fig. 2. In this event DMSP F17 crosses from high latitudes to low latitudes. (For interpretation of the references to color in this figure, the reader is referred to the web version of this article.)



**Fig. 5.** Histogram of the differences between the SECS region-1 and region-2 boundary and the DSMP/SSM region-1 and region-2 boundary for all events. Along the  $x$ -axis is the difference in geographic latitude where a negative value indicates that the SECS boundary is at a lower latitude than the DMSP boundary. The mean, median, and standard deviation are in the upper right corner.

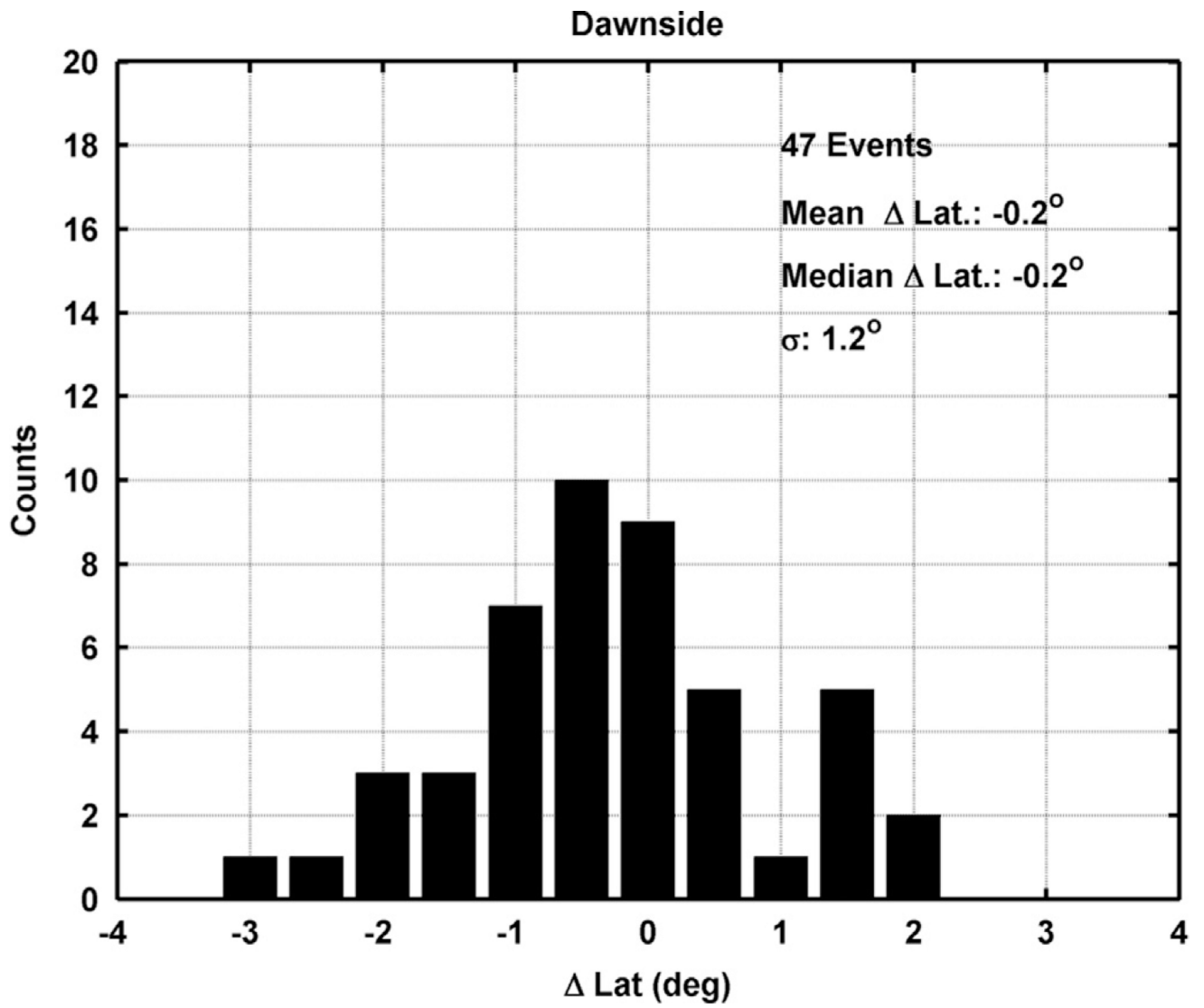


**Fig. 6.** Histogram of the differences between the SECS region-1 and region-2 boundary and the DSMP/SSM region-1 and region-2 boundary for dawnside events. This figure has the same format as Fig. 5.

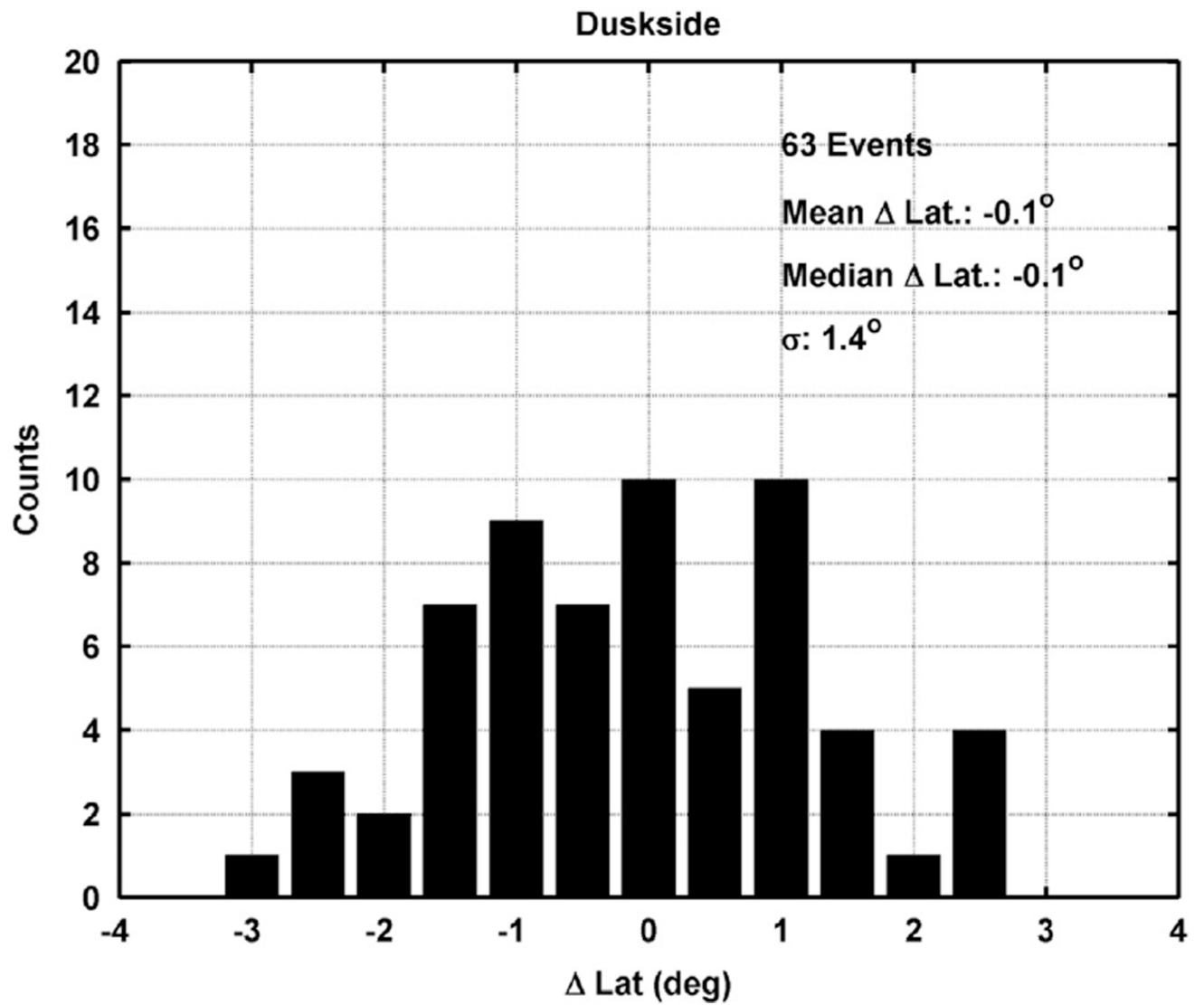


**Fig. 7.** Histogram of the differences between the SECS region-1 and region-2 boundary and the DSMP/SSM region-1 and region-2 boundary for duskside events. This figure has the same format as Fig. 5.